Green bimetallic nZVFe/Cu applied in cationic malachite green removal: linear, nonlinear, RSM, and ANN

Hossam M. Abdel-Aziz[1], Rabie S. Farag[2], Soha A. Abdel-Gawad[3]
[1]*Chemical Industries Development [CID] Company, Giza, Egypt*
[2]*Faculty of Science, Chemistry department, Al-Azhar University, Cairo, Egypt*
[3]*Faculty of Postgraduate Studies for Nanotechnology, Cairo University, Giza, Egypt*

Zero-valent iron/copper nanoparticles were effectively achieved utilizing an extract and a green synthesis technique. Dispersive X-ray spectroscopy (EDAX), Fourier transform infrared spectroscopy (FT-IR) and scanning electron microscopy (SEM) demonstrate the Ficus Benjamina nano zero-valent iron/copper FB-nZVFe/Cu synthesis. The obtained nanoparticles are between 19 and 63 nm in size. The different circumstances were examined to adjust the removal efficiency of Malachite green. Langmuir data (R^2 = 0.999), with (q_{max} = 16.33 mg g^{-1}) better fits the adsorption data. Consistent with kinetic studies, Malachite green uptake is pseudo-second order. All things considered; FB-nZVFe/Cu is a dedicated unique sensible for extracting Malachite green from solutions. When we used linear regression analysis to appraise the impacts of functional parameters, we discovered that they accounted for over 97% of the variables influencing the removal process. The data collected, and the successful analysis indicate that the FB-nZVFe/Cu green adsorbent is an intriguing material for removing Malachite green from wastewater.

Keywords: Malachite green; FB-nZVFe/Cu; Linear; Nonlinear models

ARTICLE HISTORY
Received: January 27, 2025
Revised: February 10, 2025
Accepted: February 27, 2025

CORRESPONDENCE TO
Soha A. Abdel-Gawad,
Email: soha.gawad@cu.edu.eg
DOI: 10.21608/nasj.2025.355807.1004

INTRODUCTION

Malachite green (MG) is a cationic dye solvable in water and classified as a triarylmethane dye; it is a green crystalline powder [1, 2]. In industry, MG is extensively utilized in dyeing, distilleries, and producing paints and printing inks. On the other hand, it is also most commonly used as an external antiseptic on ulcers and wounds, and not orally because it is hazardous, toxic, and may cause cancer [3]. Furthermore, it is also used as an antiseptic and fungicide to control fish disease and parasites in the aquaculture industry [4, 5]. Large volumes of Malachite green-colored wastewater are released into streams contaminated with dye from industrial finishing and dyeing processes. This causes harmful impacts on aquatic life and also affects the environment and human health [6, 7]. Among the worst contaminants in the water is Malachite green, which damages the aquatic ecosystem by lowering dissolved oxygen, blocking sunlight, and destroying the aesthetic quality of the water [8]. The detrimental effects of this dye on human health include its high toxicity and danger to mammalian cells, as well as its ability to promote liver tumors [9]. The MG dye has a molecular structure depicted in Figure 1.

To overcome these limitations, researchers have concentrated on creating novel methods utilizing nanotechnology. Fe nanoscale particles have been employed for water treatment since the 1990s due to their benefits, which include their unique adsorption, wide scattering of reactive sites, and good surface area [10, 11]. Copper nanoparticles have a large surface area, low cost, and [chemical–physical] characteristics [12-14]. Among these zero-valent metals, Cu-NPS are the most stable [15, 16]. The eradication of pollutants from aquatic environments is a significant function of nanoparticles [17, 18]. Recently, $NaBH_4$ has been used to manufacture nanoscale particles, but these particles lead to considerable contamination [10,19,20]. Conventional techniques such as vacuum sputtering, thermal decomposition, physical approach [attrition], and sonochemical synthesis were used to create Fe-NPS or Cu-NPS. Due to their numerous limitations, such as high temperatures, pressures, or energy requirements, these techniques are relatively expensive [21, 22]. Finding alternate, affordable, and ecologically friendly techniques is consequently necessary. Green synthesis is a low-cost and beneficial method for creating nanoparticles. It uses plant leaf extract its abundant in capping and reducing agents resembling flavonoids, and polyphenols, which convert iron and copper ions to zerovalent and prevent accumulation [23-25].

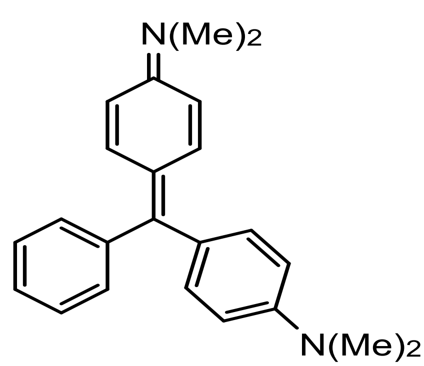

Figure 1. Malachite green molecular structure

The benefits of plants in the water treatment process include their availability, affordability, effectiveness, and non-toxicity [26-28]. A new concept for removing pollutants is Ficus Benjamina nano zerovalent iron/copper FB-nZVFe/Cu. Extracting from Ficus Benjamina leaves offers a quicker, more cost-effective, and eco-friendly way to create nanoparticles of the right size [29-31]. Green nanoparticles stop the growth of bacteria, fungi, and other microorganisms [32, 33]. Green synthesis-produced copper and iron nanoparticles have so far shown promise in eliminating a wide range of pollutants [34, 35]. Limited information has been made on the use of green synthetic iron-copper bimetallic nanoparticles despite studies showing that the green synthesis of nZVFe/Cu is feasible. Numerous investigations have demonstrated that bimetallic nanoparticles outperform monometallic ones in terms of efficiency [36, 37].

$$nFe^{+2} + nCu^{+2} + 4nAr - (OH)n \rightarrow nFe^{0} / nCu^{0} + 4nAr = O + 4nH^{+} \quad (1)$$

The simplest and most effective method for treating water is adsorption using green plant nanoparticles [38], it is also a cost-effective method. There are many different types of functional groups in it. Additionally, they don't release chemicals, are non-toxic, and have no effect on the quality of treated water. The novel concept of Ficus Benjamina-nZVFe/Cu is employed to eliminate malachite green. Thus, the target of this study is to appraise FB-nZVFe/Cu's potential for the restoration of MG-polluted water. Nanomaterials are profitable and simple to produce and have high removal efficacy.

MATERIALS AND METHODS

Chemicals

The chemicals employed were of analytical quality and high clarity. The pH was adapted by employing 0.1M HCl and 0.1M NaOH.

Synthesis of FB-nZVFe/Cu

Ficus Benjamina (FB) leaves were cleaned with tap and then distilled water to get rid of dirt; next dried in a furnace at 50°C. A 2.5 mm sieve was then used to filter the leaves after they had been chopped into tiny bits. 20 grams of leaves and 100 mL of distilled water were intermixed in an Erlenmeyer flask, heated to 60 °C for 5 minutes, and then filtered. The filtrate was then kept at 4°C until it was needed as a capping and reducing agent [39, 40]. 1.93g of $FeSO_4.2H_2O$ and 0.18g of $CuSO_4.5H_2O$ were dissolved in 100 mL of distilled water to create a solution of Fe[Ⅱ] and Cu[Ⅱ]. 50 mL of FB leaf extract supplemented to solution drop by drop with stirring for 20 minutes to synthesize FB-nZVFe/Cu nanoparticles. The development of nanoparticles was demonstrated by the solution's color changing from yellow to brown and finally black. After centrifugation for 10 minutes, distilled water and anhydrous alcohol were used to wash the FB-nZVFe/Cu particles. After being heated to 65 °C in a drier oven, FB-nZVFe/Cu was kept in a desiccator until it was needed [39-42].

Characterization technique

FT-IR spectroscopy for multi-functional group analysis, EDAX, and SEM (JEOL-JSM-5410, Japan) was utilized to explore the morphological surface of FB-nZVFe/Cu sample.

Batch adsorption studies

In batch adsorption, 0.4 g L^{-1} of FB-nZVFe/Cu was mixed with MG solution at 5, 10, 15, and 20 mg L^{-1} at λ_{max} 617 nm to assess the removal process. The MG removal was estimated utilizing the ensuing formula:

$$Sorption\,[\%] = [Co - Ce]/Co \times 100 \quad (2)$$

where C_0 and C_e, are the MG starting and equilibrium concentration (mg L^{-1}). The adsorption capability of MG was identified utilizing the subsequent formula.

$$q_e\,[mg\,g^{-1}] = [[C_o - C_e]\,V]/\,m \quad (3)$$

where V is the solution volume (L), m is the adsorbent weight (g), and q_e is the adsorption capability (mg g^{-1})[43].

Adsorption isotherms study

Freundlich is an experiential computation utilized for stamping multilayered dissimilar surfaces and is donated by this equation [44]:

$$Ln\,qe = 1/n\,ln\,Ce + ln\,Kf \quad (4)$$

Adsorption intensity and capacity are measured by the Freundlich constants n (dimensionless) and K_f ((mg g^{-1}) (mg L^{-1})$^{1/n}$) and computed using the intercept and slope values of the graph of ln C_e vs. ln q_e.

This equation provides Langmuir's estimate of the smooth mono-layer of MG across an adsorbent surface [45]:

$$C_e / q_e = 1 / [K_L\,q_{max}] + C_e/q_{max} \quad (5)$$

Where q_e (mg g^{-1}) is the quantity of dye absorbed /mass of employed adsorbent and C_e (mg L^{-1}) is the dye equilibrium concentration. The maximal monolayer adsorption capacity, q_{max} (mg g^{-1}), and K_L (L mg^{-1}) were acquired utilizing the slope and intercept of the graph of C_e vs C_e/q_e.

Kinetic study

Pseudo-first-order (PFO) and pseudo-second-order (PSO) kinetic models were utilized to explain the behavior of solid-liquid systems at various contact times, such as 15, 30, 45, 69, 90, and 120 minutes by 0.4 g L^{-1} of adsorbent, pH 8, and 100 rpm of stirring [39, 40].

The PFO utilized to designate the adsorption rate, which is stated as follows:

$$\ln[qe\text{-}qt] = \ln qe - K1\ t \qquad (6)$$

The plot of ln (q_e-q_t) against t yields the first-order equilibrium constant K_1, and the concentration of the dye's adsorption values in media at equilibrium and at time t is (q_e and q_t).

The most widely utilized and simplified kinetic equations are PSO equations. The following is a typical description of the pseudo-second-order kinetic model:

$$t/qt\ =\ 1/\ K2qe2 + t/qe \qquad (7)$$

where K_2 (g/mg.min) represents the adsorption rate constant and q_e and q_t (mg g^{-1}) represent the adsorption capacities at equilibrium and time t (min), respectively. Drawing t/qt versus t is the method used to determine K_2 values.

Reusability study

The adsorbent's reusability is a crucial aspect in determining its cost-effectiveness and meeting both ecological and economic demands. MG was absorbed into FB-nZVFe/Cu at a concentration of 10 mgL^{-1}. The studies were replicated up to five times by subjecting FB-nZVFe/Cu to a new MG solution to investigate reusability further. Before being utilized for the subsequent adsorption recycling, the FB-nZVFe/Cu was always extracted from the medium by centrifugation for 10 min, cleaned with ethanol, and dried in a furnace at 45 °C.

Statistical analysis utilizing Linear modeling algorithms

IBM SPSS Statistics 24 was utilized to do a linear regression analysis to inspect the influence of diverse operating factors. The ANOVA program displayed the sum of squares and the overall model's impact. If the P value is less than 0.05, the model is regarded are successful [46, 47].

Response Surface Methodologies [RSM] The influence of varying working settings was assessed, and the results obtained validate the practical findings. The effect is considered significant for the removal process if the P value is less than 0.05; if the P value is more than 0.05, the effect is respected as not significant. Equation 8 can be used to infer the removal equation:

$$R\ \% = Bo + B_1X_1 + B_2X_2 + B_3X_3 + B_4X_4 + B_5X_5 \quad (8)$$

The variables X_1, X_2, X_3, X_4, and X_5 represent the influences of pH, contact duration, adsorbent dosage, stirring rate, and concentration, respectively; B_0 is a constant; and R is the removal percentage [48, 49].

Artificial neural network [ANN] To estimate the removal efficacies of wastewater contaminants, an artificial neural network [ANN] with input, hidden, and output layers called "Multilayer Perceptron Backpropagation [MLPB]" was created. One of the neural network topologies that is most frequently utilized is multilayer perception. The hidden layer held several neurons, whereas the input layer received data from the five testing aspects (pH, contact time, amount of adsorbent, stirring speed, and beginning concentration). Trial and error were used to determine the number of neurones and hidden layers. Typically, all accessible data is separated into standard values for testing methods [20%], validation [20%], and training [60%]. Through an ongoing simulation process, the ANN's link weight and bias are adjusted through network training. To change the weights and biases, the mean squared error [MSE], which traveled back from the output layer to the input layer, was calculated by comparing the output with the target. ANN models that use backpropagation show the significance and normalized significance of each covariable in addition to the link concerning trained and tested values [50].

RESULTS AND DISCUSSION

Characterization of FB-nZVFe/Cu

SEM and EDAX Fiscus Benjamina-nZVFe/Cu particles have a semi-spherical form and span in size from about 19 to 63 nm, consistent with the SEM image. As seen in Figure 2, numerous pores enhance the MG removal procedure. Bimetallic nZVFe/Cu particle synthesis is indicated by EDAX analysis. The presence of bimetallic is shown by the Fe and Cu peaks. Figure 3 displays additional peaks of the fiscus extract, like C, O, Si, and S [39, 41].

FT-IR measurements The FT-IR spectra of FB-nZVFe/Cu before the reaction is displayed in Figure 4 and fall between 400 and 4000 cm^{-1}. The incidence of

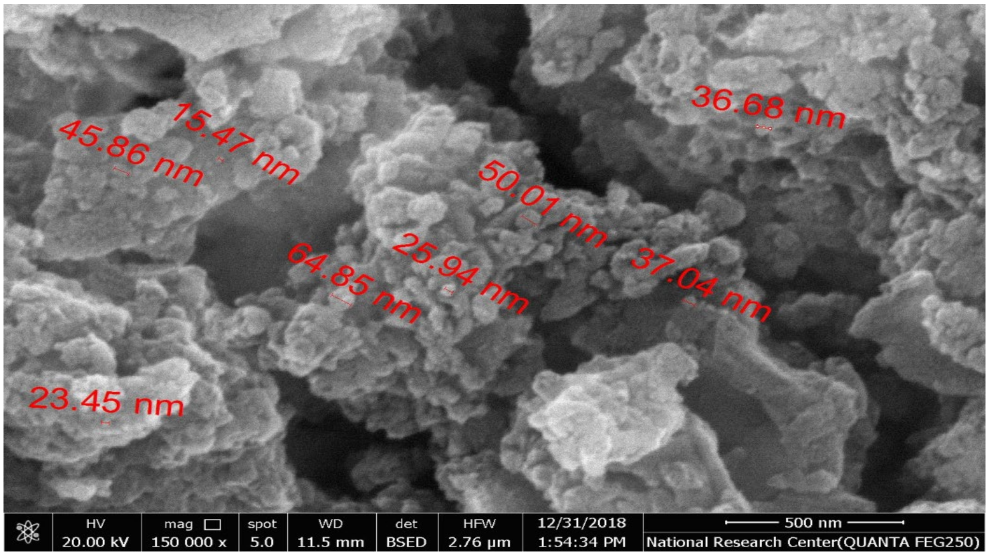

Figure 2. SEM of FB-nZVFe/Cu sample

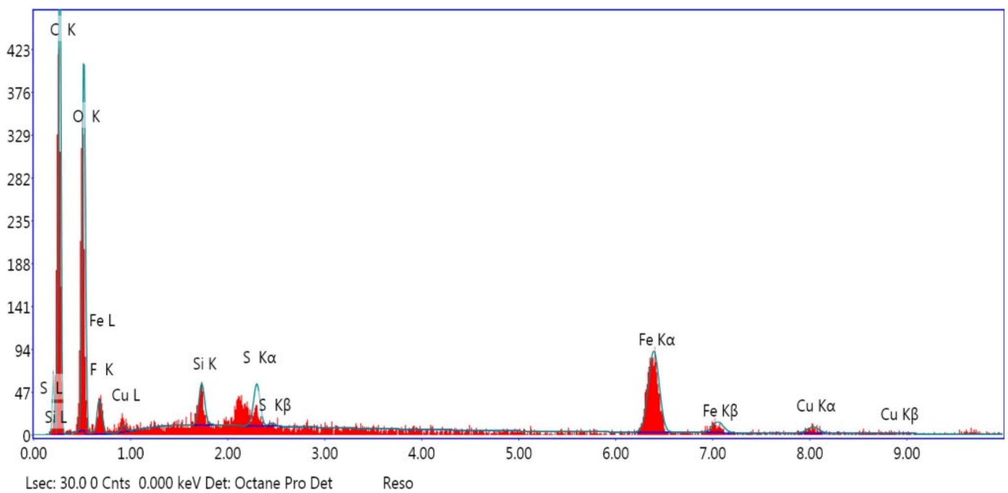

Figure 3. EDAX of prepared FB-nZVFe/Cu sample

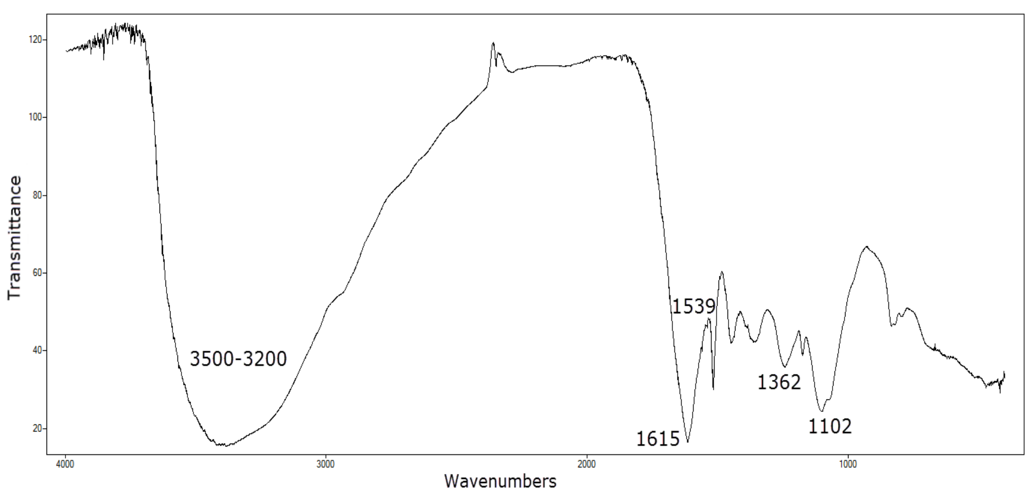

Figure 4. FT-IR spectrum prepared FB-nZVFe/Cu sample

polyphenols, which might increase material stability, are indicated by the bandwidth at 3400 to 3000 cm^{-1}, which was ascribed to the O-H band [13, 39, 51]. The band of C=O was detected at 1615 cm^{-1}[51, 52]; Ficus amide was found at 1539 cm^{-1} [42, 53, 54]; polyphenols' aromatic ring C=C stretched vibration was found at 1362 cm^{-1}[12, 40, 53]; and C-O-C symmetric stretched vibration was found at 1102 cm^{-1}[55, 56]. Figure 4 displays the survival and intensity of phenolic compound peaks, which are a reliable indicator of synthesized FB-nZVFe/Cu [39-42].

Effect of operational parameters

Effect of pH The pH procedure, which regulates adsorbent surface charge and capacity as well as adsorbate solubility qualities via alkalinity or acidity, is the utmost crucial in the MG elimination process. The effectiveness of MG elimination at various pH levels 4, 6, 8, and 10, as exemplified in Figure 5, the elimination efficiency was 19, 30, 57, and 48% as FB-nZVFe/Cu dose was 0.4 g L^{-1}, the concentration was 10 mg L^{-1}, and the stirring was 100 rpm. It was perceived that pH 8 is the best proper for the MG removal. The zero charge point of Ficus Benjamina is a low 4.85 [57]. The positively charged surface of FB-nZVFe/Cu caused repulsion with Malachite green at pH< pH_{pzc} (At pH4), resulting in low removal effectiveness. Additionally, the removal will be significantly diminished at a higher pH (pH10) since a significant portion of the material will precipitate in the solution. Maximum Malachite green elimination occurs at pH 8 owing to the attraction between negatively charged FB-nZVFe/Cu and positively charged MG, as well as a large number of available unoccupied sites that interfere with the bimetallic nanoparticles and the contaminant [58, 59].

The effects of contact time Utilizing 0.4 g L^{-1} of FB-nZVFe/Cu at pH 8, the effects of various times 30, 45, 60, 90, and 120 minutes on the removal of Malachite green 10 mg L^{-1} were investigated. The stirring rate was set at 100 rpm, and the removal percentage was 52.57, 62, 63, 64, and 64%, as depicted in Figure 6. Gradually increasing the contact time increased the number of molecules created by the electrical attraction between negatively charged FB-nZVFe/Cu and positively charged MG molecules, increasing the concentration of pollutants in the empty spaces of the nanoparticles. The effectiveness with which the MG dye is removed increases when the contact time interval increases, reaching a maximum and remaining relatively constant. A contact time of 45 minutes results in the highest % of elimination.

Effect of adsorbent dosage The efficacy of removing Malachite green was assessed related to the dose impact of the adsorbents, which varied from 0.3 to 0.6 g L^{-1}, as well as other operational factors, 45 minutes and a pH of 8. As seen in Figure 7, the ideal adsorbent dosage for removing Malachite green was determined to designate around 0.4 g L^{-1}. The concentration of MG is 10 mg L^{-1}, and the removal percentages were 44, 62, 76, and 90%. As anticipated, the number of unoccupied sites increases with rising FB-nZVFe/Cu dosage, followed by an increase in removal.

Effect of stirring rate The removal of MG by FB-nZVFe/Cu as an indication of the stirring rate is demonstrated in Figure 8. The stirring rate was adjusted between 100 and 250 rpm, pH 8 and time of 45 minutes. The removal ratios were 62, 63, 63, and 63 percent, while the MG concentration was 10 mg L^{-1}. 100 rpm was determined to be the ideal stirring rate for MG removal.

Effect of the concentration Ficus-ZVFe/Cu particle removal tests were conducted on MG solutions with varying concentrations 5, 10, and 15 mgL^{-1}, at pH 8, for 45 minutes and with an adsorbent dosage of 0.4 g L^{-1}. The removal was 89, 62, 43, and 32 %, as seen in Figure 9. Due to the presence of many vacant adsorption sites, which are big about the pollutant concentration, and the percentage of removal without rising concentration, the removal ratio is high at low concentrations at the start of the study.

Adsorption isotherm

The two most popular isotherms applications, Freundlich and Langmuir isotherms, predict and estimate the adsorption capability of FB-nZVFe/Cu, as illustrated in Figures 10–12. According to Table 1, Langmuir model had a maximum adsorption capability of 16.33 mg g^{-1} and was well fitted with isotherms in both linear and non-linear forms by having better determination coefficients R^2 and a lower error total than Freundlich.

Kinetics studies

As illustrated in Figures 13–15, Table 2 demonstrates that PSO model fits the data more accurately than PFO, both linearly and non-linearly. For Malachite green, the value q_e [cal]= 16.99 is almost equivalent to q_e [exp]= 16.2. The findings indicate that the PSO is being followed by MG absorption on FB-nZVFe/Cu.

Statistical analysis

After calculating the impact of the subsequent variables on the removal strategy, R^2 = 0.980 was

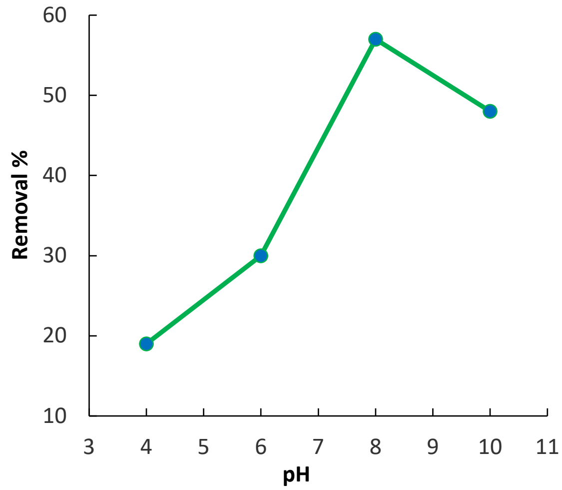

Figure 5. Effect of pH on Malachite green removal

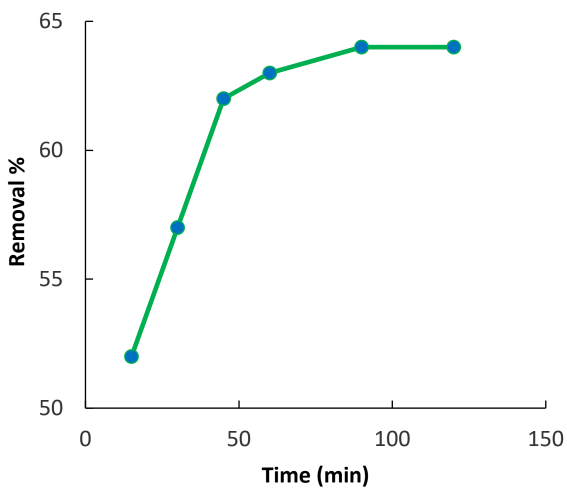

Figure 6. Effect of contact time on Malachite green removal

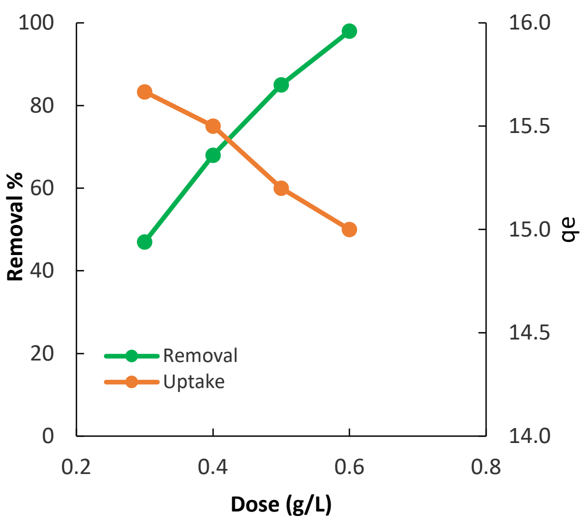

Figure 7. The optimum dose and uptake for Malachite green removal

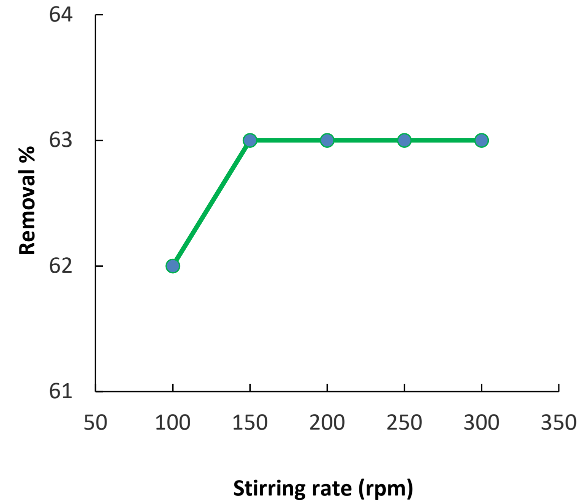

Figure 8. Effect of stirring rate on Malachite green removal

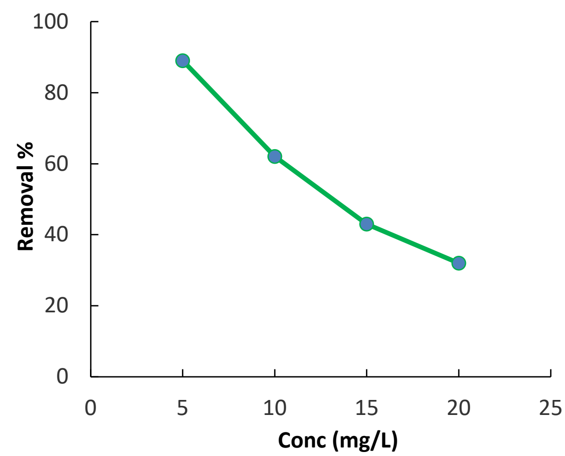

Figure 9. Effect of concentration on Malachite green removal

Table 1. Isotherm models for removal of Malachite green

Parameters	Freundlich	Langmuir
	Kf= 12.30 **n**= 8.311	**Q_o**= 16.33 **b**= 2.796
	- Linear	
R^2	0.91	0.999
	- Non-Linear	
Errors:		
CHI	0.1884	0.1306
ERRSQ	2.0534	1.9630
HYBRD	0.1703	0.1277
MPSD	0.0144	0.0084
ARE	0.1811	0.1619
EABS	2.3436	2.4176
Error sum	**4.9512**	**4.8092**

.

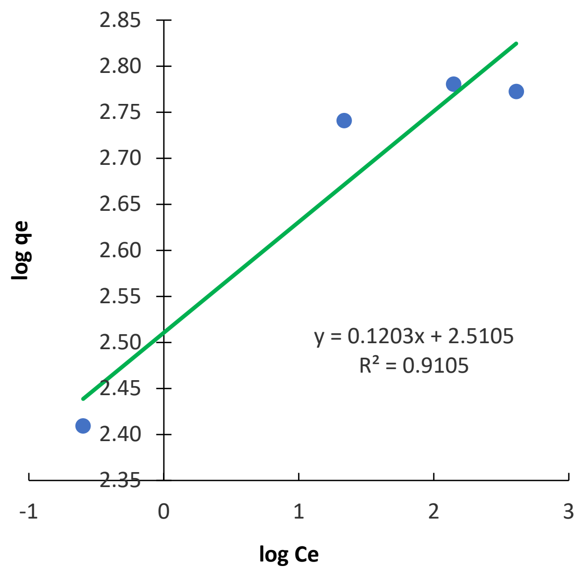

Figure 10. Freundlich for Malachite green contributing component

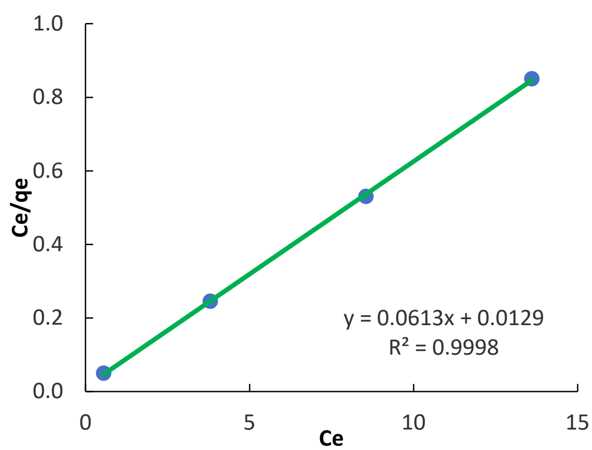

Figure 11. Langmuir for Malachite green contributing component

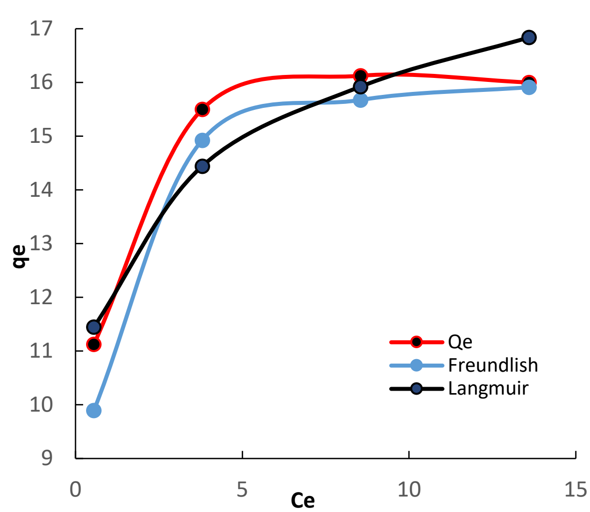

Figure 12. Isotherm studies for nonlinear models

Table 2. Kinetic models for the removal of Malachite green

Parameters	PFO	PSO
	Qe= 7.94 **K_1**= 0.058	**Qe**= 16.63 **K_2**= 0.015
	- Linear	
R^2	0.978	0.999
	- Non-Linear	
Errors:		
CHI	0.265	0.018
ERRSQ	6.704	0.270
HYBRD	1.847	0.019
MPSD	0.129	0.001
ARE	0.709	0.064
EABS	10.289	0.934
Error sum	**19.943**	**1.307**

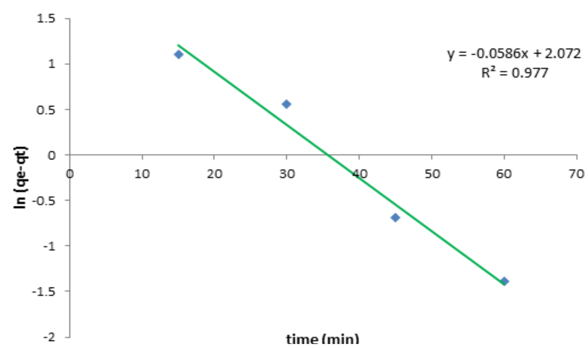

Figure 13. The PFO kinetics model for Malachite Green

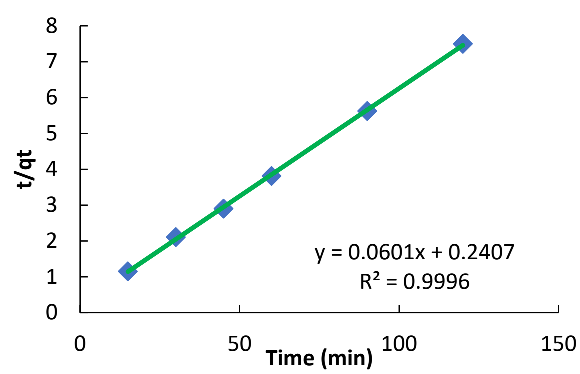

Figure 14. The PSO kinetics model for Malachite green

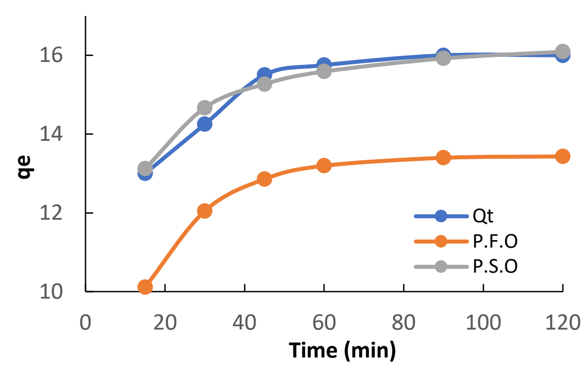

Figure 15. Kinetic studies for nonlinear models.

determined. Given the extremely low estimate error (3.61299), this indicates that the variables under study accounted for over 98% of all the elements influencing the process. The data provided by the ANOVA program demonstrated that the model is successful when the P value is less than 0.05.

Response Surface Methodologies (RSM) Utilizing linear regression analysis (IBM-SPSS Statistics), the implication of several considerations was inspected; the findings corroborate the empirical findings. All factors had an impact on the removal approach, according to the data in Table 3. However, the stirring rate's effect was deemed to be insignificant when the P value was more than 0.05, meaning it could be disregarded during the removal process. The removal equation can be inferred by using the B values displayed in Table 3, which are as follows:

$$R\% = B_o + B_1X_1 + B_2X_2 + B_3X_3 + B_4X_4 + B_5X_5 \quad (8)$$

$$= 64.972 + (-4.924)\,X1 + (0.295)\,X2 + (145.764)\,X3 + (0.006)\,X4 + (-3.551)\,X5$$

The variables X_1, X_2, X_3, X_4, and X_5 represent different variables in the given equation. They include the effects of pH (4, 6, 8, and 10), contact time (15, 30, 45, 60, 90, 120, and 150 min), adsorbent dose (0.3, 0.4, 0.5, and 0.6 g L^{-1}), stirring rate (100, 150, 200, 250, and 300 rpm), and concentration (5, 10, 15, and 20 mg L^{-1}).

Artificial neural network

The Multilayer Perceptron neural network model 6-4-1 was used to train the ANN model. Sample training and testing were used for MG removal, with no results excluded. A total of 24 runs were directed, with the sum of squares errors for training and testing of 0.727 and 0.632, respectively, and relative errors of 0.090 and 0.126. To advance the artificial intelligence of the output layer (elimination percentage), Figure 16 displays neural network models with five covariables as input layers coupled in a hidden layer and bias. The normalized value and the predicted values differ slightly, as seen in Figure 17. Figure 18 illustrates the actuality of the result and the efficacy of the model results in defining the adsorption of MG onto the FB-nZVFe/Cu surface by showing a slight discrepancy between the residual value and the prediction value (-10, 10%). Figure 19 illustrates the significance of each covariable in the removal efficiency, revealing that stirring rate was the least effective parameter and pH was the most effective. The normalized importance is reliable with analyses of impact of RSM statistical algorithm and operational parameter.

Table 3. Malachite green statistical analysis

Model	B	Sig.
(Constant)	64.972	0.008
pH	-4.924	0.030
Time	0.295	0.014
Dose	145.764	0.000
Stirring	0.006	0.775
Concentration	-3.551	0.000

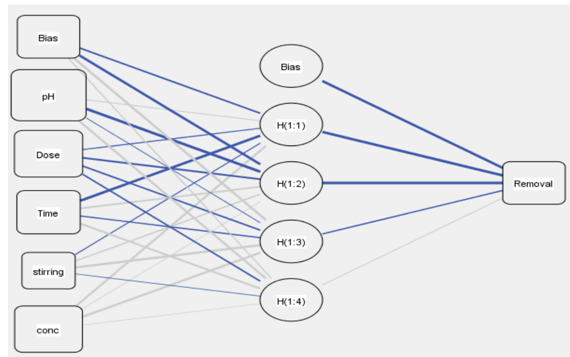

Figure 16. Malachite green multilayer perceptron neural network

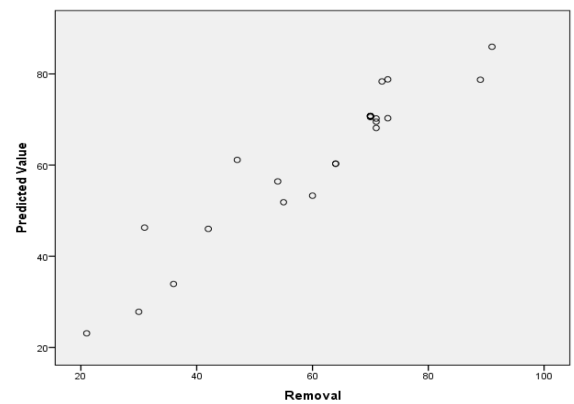

Figure 17. Malachite green predictive values

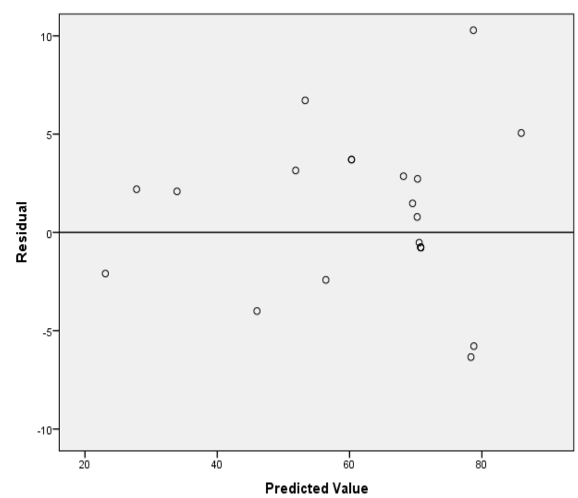

Figure 18. Malachite green residual values

The ANN outcomes were in concord with experimental data and RSM results.

Reusability study

As shown in Figure 20, removal efficiency is reduced with each round of remedies. Therefore, after being utilized up to five recycles, respectively, the removal efficiency was 60, 58, 55, 53, and 51%. Even after the fifth recycling, MG's elimination efficiency remained strong. The reduction in removal suitability may have been brought on by an irreversible filling of adsorption sites or by the loss of nano-absorbent. After five recycling cycles, the regenerated adsorbent still had good adsorption capacity. According to these findings, green-nZVFe/Cu has a great chance of being employed frequently to remove MG without noticeably lowering removal suitability.

Finally, the outcomes obtained indicate that FB-nZVFe/Cu is an ecological adsorbent that effectively removes Malachite green dye from wastewater and yields high-quality handled effluent after five recycles.

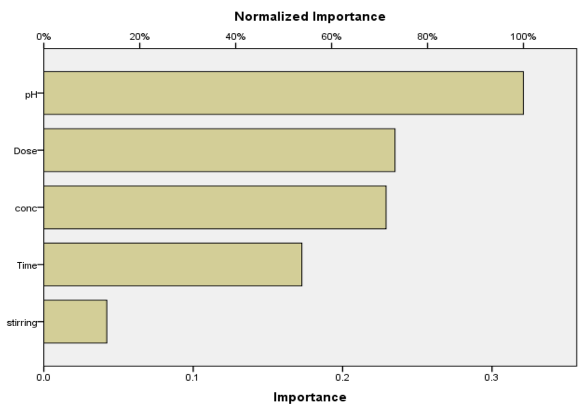

Figure 19. Malachite green importance for each covariable

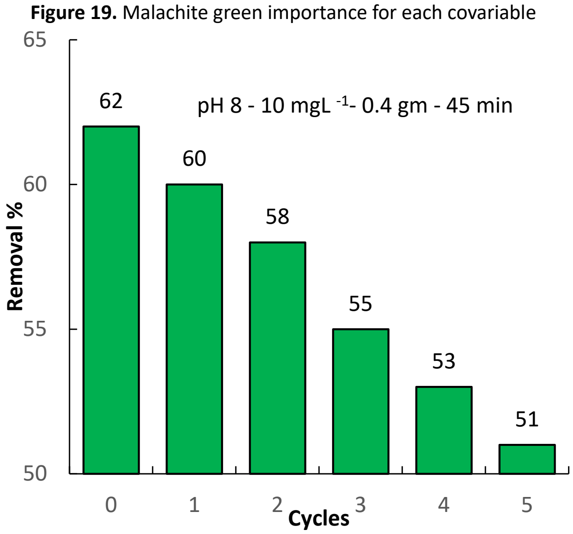

Figure 20. Reusability cycles

CONCLUSIONS

Green zero-valent Fe/Cu nanoparticles are used in this study to remove MG under a variety of operating conditions. At pH 8, the maximum amount of MG was eliminated. With 0.4 g L^{-1} of FB-nZVFe/Cu, a stirring rate of 100 rpm, a pH of 8, and a contact time of 45 minutes, the removal efficiency was between 89 and 32% when Malachite Green was used at concentrations of 5, 10, 15, and 20 mg L^{-1}. The removal efficacy rose by 46% (C_0 = 10 mg L^{-1}) when the dose was raised from 0.3 to 0.6 mg L^{-1}. A more significant correlation coefficient (R^2 = 0.999) with q_{max} = 16.33 mg g^{-1} designates that Langmuir model is more proper with the isotherm. With a greater R^2 than PFO, the PSO model better fits the kinetic model data. The study's findings indicate no distinction between linear and non-linear models. After five uses, the substance still operates well, removing more than 50% of the material. Ficus Benjamin is used to create iron and copper nanoparticles in a green way. This substitutional process is environmentally beneficial and can result in high-quality treated wastewater.

REFERENCES

[1] N.P. Raval, P.U. Shah, N.K. Shah, Malachite green "a cationic dye" and its removal from aqueous solution by adsorption, Applied Water Science, 7 (2017) 3407-3445.

[2] N.P. Raval, P.U. Shah, N.K. Shah, Nanoparticles loaded biopolymer as effective adsorbent for adsorptive removal of malachite green from aqueous solution, Water Conservation Science and Engineering, 1 (2016) 69-81.

[3] W. Cheng, S.-G. Wang, L. Lu, W.-X. Gong, X.-W. Liu, B.-Y. Gao, H.-Y. Zhang, Removal of malachite green (MG) from aqueous solutions by native and heat-treated anaerobic granular sludge, Biochemical engineering journal, 39 (2008) 538-546.

[4] J. Trujillo-Reyes, V. Sánchez-Mendieta, M. José Solache-Ríos, A. Colín-Cruz, Removal of remazol yellow from aqueous solution using Fe–Cu and Fe–Ni nanoscale oxides and their carbonaceous composites, Environmental technology, 33 (2012) 545-554.

[5] E.J. Lara-Vásquez, M. Solache-Ríos, E. Gutiérrez-Segura, Malachite green dye behaviors in the presence of biosorbents from maize (Zea mays L.), their Fe-Cu nanoparticles composites and Fe-Cu nanoparticles, Journal of Environmental Chemical Engineering, 4 (2016) 1594-1603.

[6] M.-H. Baek, C.O. Ijagbemi, O. Se-Jin, D.-S. Kim, Removal of Malachite Green from aqueous solution using degreased coffee bean, Journal of hazardous materials, 176 (2010) 820-828.

[7] B. Hameed, M. El-Khaiary, Batch removal of malachite

green from aqueous solutions by adsorption on oil palm trunk fibre: equilibrium isotherms and kinetic studies, Journal of hazardous materials, 154 (2008) 237-244.

[8] M. Amiri, M. Salavati-Niasari, A. Akbari, T. Gholami, Removal of malachite green (a toxic dye) from water by cobalt ferrite silica magnetic nanocomposite: herbal and green sol-gel autocombustion synthesis, international journal of hydrogen energy, 42 (2017) 24846-24860.

[9] Z. Bekçi, Y. Seki, L. Cavas, Removal of malachite green by using an invasive marine alga Caulerpa racemosa var. cylindracea, Journal of hazardous materials, 161 (2009) 1454-1460.

[10] C. Devatha, A.K. Thalla, S.Y. Katte, Green synthesis of iron nanoparticles using different leaf extracts for treatment of domestic waste water, Journal of cleaner production, 139 (2016) 1425-1435.

[11] T. Wang, X. Jin, Z. Chen, M. Megharaj, R. Naidu, Green synthesis of Fe nanoparticles using eucalyptus leaf extracts for treatment of eutrophic wastewater, Science of the total environment, 466 (2014) 210-213.

[12] J.B. Fathima, A. Pugazhendhi, M. Oves, R. Venis, Synthesis of eco-friendly copper nanoparticles for augmentation of catalytic degradation of organic dyes, Journal of Molecular Liquids, 260 (2018) 1-8.

[13] N. Nazar, I. Bibi, S. Kamal, M. Iqbal, S. Nouren, K. Jilani, M. Umair, S. Ata, Cu nanoparticles synthesis using biological molecule of P. granatum seeds extract as reducing and capping agent: Growth mechanism and photo-catalytic activity, International journal of biological macromolecules, 106 (2018) 1203-1210.

[14] M.A. Zayed, S.A. Abdel-Gawad, H.M. Abdel-Aziz, Green synthesis of zero-valent copper nanoparticles for removal of D-yellow 119 textile dye from aqueous medium, Environmental Progress & Sustainable Energy, 43 (2024) e14473.

[15] J. Zhang, J. Guo, Y. Wu, Y. Lan, Y. Li, Efficient activation of ozone by zero-valent copper for the degradation of aniline in aqueous solution, Journal of the Taiwan Institute of Chemical Engineers, 81 (2017) 335-342.

[16] M. Nasrollahzadeh, M. Sajjadi, H.R. Dasmeh, S.M. Sajadi, Green synthesis of the Cu/sodium borosilicate nanocomposite and investigation of its catalytic activity, Journal of Alloys and Compounds, 763 (2018) 1024-1034.

[17] T. Tatarchuk, I. Mironyuk, V. Kotsyubynsky, A. Shyichuk, M. Myslin, V. Boychuk, Structure, morphology and adsorption properties of titania shell immobilized onto cobalt ferrite nanoparticle core, Journal of Molecular Liquids, 297 (2020) 111757.

[18] N. Nagar, V. Devra, Green synthesis and characterization of copper nanoparticles using Azadirachta indica leaves, Materials chemistry and physics, 213 (2018) 44-51.

[19] A.S. Mahmoud, M.M. El-Tayieb, N.A.S. Ahmed, A.M. Mostafa, Algorithms and statistics for municipal wastewater treatment using nano zero valent iron (nZVI), Journal of Environment & Biotechnology Research, 7 (2018) 30-44.

[20] C. Balalakshmi, K. Gopinath, M. Govindarajan, R. Lokesh, A. Arumugam, N.S. Alharbi, S. Kadaikunnan, J.M. Khaled, G. Benelli, Green synthesis of gold nanoparticles using a cheap Sphaeranthus indicus extract: impact on plant cells and the aquatic crustacean Artemia nauplii, Journal of Photochemistry and Photobiology B: Biology, 173 (2017) 598-605.

[21] M. Danish, X. Gu, S. Lu, A. Ahmad, M. Naqvi, U. Farooq, X. Zhang, X. Fu, Z. Miao, Y. Xue, Efficient transformation of trichloroethylene activated through sodium percarbonate using heterogeneous zeolite supported nano zero valent iron-copper bimetallic composite, Chemical engineering journal, 308 (2017) 396-407.

[22] X. Weng, M. Guo, F. Luo, Z. Chen, One-step green synthesis of bimetallic Fe/Ni nanoparticles by eucalyptus leaf extract: Biomolecules identification, characterization and catalytic activity, Chemical Engineering Journal, 308 (2017) 904-911.

[23] Y. Liu, X. Jin, Z. Chen, The formation of iron nanoparticles by Eucalyptus leaf extract and used to remove Cr (VI), Science of the Total Environment, 627 (2018) 470-479.

[24] D.A. Selvan, D. Mahendiran, R.S. Kumar, A.K. Rahiman, Garlic, green tea and turmeric extracts-mediated green synthesis of silver nanoparticles: Phytochemical, antioxidant and in vitro cytotoxicity studies, Journal of Photochemistry and Photobiology B: Biology, 180 (2018) 243-252.

[25] H.M. Abd El-Aziz, M.A. Zayed, S.A. Abdel-Gawad, Adsorptive removal of Direct Red 31 and Direct Orange 26 azo dyes from aqueous solutions using Ficus nano zero valent copper: Linear, non-linear, response surface methodology (RSM), and artificial neural network (ANN) modeling, Adsorption Science & Technology, 42 (2024) 02636174241256849.

[26] M. Shanehsaz, S. Seidi, Y. Ghorbani, S.M.R. Shoja, S. Rouhani, Polypyrrole-coated magnetic nanoparticles as an efficient adsorbent for RB19 synthetic textile dye: Removal and kinetic study, Spectrochimica Acta Part A: Molecular and Biomolecular Spectroscopy, 149 (2015) 481-486.

[27] M. Fazlzadeh, K. Rahmani, A. Zarei, H. Abdoallahzadeh, F. Nasiri, R. Khosravi, A novel green synthesis of zero valent iron nanoparticles (NZVI) using three plant extracts and their efficient application for removal of Cr (VI) from aqueous solutions, Advanced Powder Technology, 28 (2017) 122-130.

[28] M. Ismail, M. Khan, S.B. Khan, M.A. Khan, K. Akhtar, A.M. Asiri, Green synthesis of plant supported CuAg and CuNi bimetallic nanoparticles in the reduction of nitrophenols and organic dyes for water treatment, Journal of Molecular Liquids, 260 (2018) 78-91.

[29] C. Puente, I. Gómez, B. Kharisov, I. López, Selective colorimetric sensing of Zn (II) ions using green-synthesized silver nanoparticles: Ficus benjamina extract as reducing and stabilizing agent, Materials

Research Bulletin, 112 (2019) 1-8.
[30] K.M. Al-Qahtani, Cadmium removal from aqueous solution by green synthesis zero valent silver nanoparticles with Benjamina leaves extract, The Egyptian Journal of Aquatic Research, 43 (2017) 269-274.
[31] M.A. Zayed, S.A. Abdel-Gawad, H.M. Abdel-Aziz, Z.A. Abo-Ayad, Green synthesis of nano-zero-valent copper for the D-blue 60 textile dye removal from aqueous medium, International Journal of Environmental Research, 17 (2023) 12.
[32] G. Rathi, S. Siddiqui, S. Chaudhry, Green material from plant source for the remediation of Methylene Blue dye: An emerging wastewater treatment technology, Handbook of Textile Effluent Remediation. New York: Pan Stanford, (2018).
[33] S. Dhuper, D. Panda, P. Nayak, Green synthesis and characterization of zero valent iron nanoparticles from the leaf extract of Mangifera indica, Nano Trends: J Nanotech App, 13 (2012) 16-22.
[34] J. Cao, R. Xu, H. Tang, S. Tang, M. Cao, Synthesis of monodispersed CMC-stabilized Fe–Cu bimetal nanoparticles for in situ reductive dechlorination of 1, 2, 4-trichlorobenzene, Science of the Total Environment, 409 (2011) 2336-2341.
[35] P. Sepúlveda, M.A. Rubio, S.E. Baltazar, J. Rojas-Nunez, J.S. Llamazares, A.G. Garcia, N. Arancibia-Miranda, As (V) removal capacity of FeCu bimetallic nanoparticles in aqueous solutions: The influence of Cu content and morphologic changes in bimetallic nanoparticles, Journal of colloid and interface science, 524 (2018) 177-187.
[36] N. Qin, Y. Zhang, H. Zhou, Z. Geng, G. Liu, Y. Zhang, H. Zhao, G. Wang, Enhanced removal of trace Cr (VI) from neutral and alkaline aqueous solution by FeCo bimetallic nanoparticles, Journal of colloid and interface science, 472 (2016) 8-15.
[37] Q. Liu, X. Yan, Q. Lai, X. Su, Bimetallic gold/silver nanoclusters-gold nanoparticles based fluorescent sensing platform via the inner filter effect for hyaluronidase activity detection, Sensors and Actuators B: Chemical, 282 (2019) 45-51.
[38] N.K. Abdulla, S.I. Siddiqui, N. Tara, A.A. Hashmi, S.A. Chaudhry, Psidium guajava leave-based magnetic nanocomposite γ-Fe2O3@ GL: a green technology for methylene blue removal from water, Journal of Environmental Chemical Engineering, 7 (2019) 103423.
[39] Hossam_M., Carbamazepine Removal from Aqueous Solution by Green Synthesis Zero-Valent Iron/Cu Nanoparticles with Ficus Benjamina Leaves' Extract, International Journal of Environmental Research, 13 (2019) 843-852.
[40] Hossam_M., Removal of caffeine from aqueous solution by green approach using Ficus Benjamina zero-valent iron/copper nanoparticles, Adsorption Science & Technology, (2020) 0263617420947495.
[41] Abdel-Aziz, Paracetamol removal by bimetallic zero-valent Fe/Cu with benjamina leaf extract, Journal of Environmental Engineering and Science, (2020) 1-11.
[42] Hossam_M., Removal of contaminant metformin from water by using Ficus benjamina zero-valent iron/copper nanoparticles, Nanotechnology for Environmental Engineering, 4 (2020) 23.
[43] S.A.A.-G. Hossam M Abdel-Aziz, Removal of sunset YellowAzo dye using activated carbon entrapped in alginate from aqueous solutions, Open Access Journal of Science, 4 (2020) 1–6.
[44] Soha_A., Adsorption Study for Chemical Oxygen Demand Removal from Aqueous Solutions using Alginate Beads with Entrapped Activated Carbon, Journal of Indian Water Resources Society, 37 (2017) 461-470.
[45] Soha_A., Effective removal of chemical oxygen demand and phosphates from aqueous medium using entrapped activated carbon in alginate, MOJ Biology and Medicine, 3 (2018) 227–236.
[46] Abdel-Gawad, Removal of ethinylestradiol by adsorption process from aqueous solutions using entrapped activated carbon in alginate biopolymer: isotherm and statistical studies, Applied Water Science, 9 (2019) 75.
[47] S.A. Abdel–Gawad, H.M. Abd El–Aziz, Removal of Pharmaceuticals From Aqueous Medium Using Entrapped Activated Carbon in Alginate, Air, Soil and Water Research, 12 (2019) 1178622119848761.
[48] Abdel-Aziz, Removal of Orange G by Fenton and Ficus Benjamina nano Zero Valent Iron, Journal of Environmental Engineering and Science, (2020) 1-10.
[49] Abdel-Aziz, Removal of inorganic contaminant phosphate from aqueous solutions by bimetallic Ficus-ZVFe/Cu nanoparticles, International Journal of Environmental Engineering, 11 (2021) 53-68.
[50] A.S. Mahmoud, R.S. Farag, M.M. Elshfai, Reduction of organic matter from municipal wastewater at low cost using green synthesis nano iron extracted from black tea: Artificial intelligence with regression analysis, Egyptian Journal of Petroleum, (2019).
[51] D.A. Demirezen, Y.Ş. Yıldız, Ş. Yılmaz, D.D. Yılmaz, Green synthesis and characterization of iron oxide nanoparticles using Ficus carica (common fig) dried fruit extract, Journal of bioscience and bioengineering, 127 (2019) 241-245.
[52] S. Yousef, M. Tatariants, V. Makarevičius, S.-I. Lukošiūtė, R. Bendikiene, G. Denafas, A strategy for synthesis of copper nanoparticles from recovered metal of waste printed circuit boards, Journal of cleaner production, 185 (2018) 653-664.
[53] F. Zhu, S. Ma, T. Liu, X. Deng, Green synthesis of nano zero-valent iron/Cu by green tea to remove hexavalent chromium from groundwater, Journal of Cleaner Production, 174 (2018) 184-190.
[54] K. Ramesh Kumar, G.P. Nattuthurai, T. Mariappan, Biosynthesis of silver nanoparticles from Morinda tinctoria leaf extract and their larvicidal activity against Aedes aegypti Linnaeus 1762, J Nanomed Nanotechnol, 5 (2014) 2.

[55] M.A. Asghar, E. Zahir, S.M. Shahid, M.N. Khan, M.A. Asghar, J. Iqbal, G. Walker, Iron, copper and silver nanoparticles: Green synthesis using green and black tea leaves extracts and evaluation of antibacterial, antifungal and aflatoxin B1 adsorption activity, Lwt, 90 (2018) 98-107.
[56] N.S.A. Mubarak, A.H. Jawad, W. Nawawi, Equilibrium, kinetic and thermodynamic studies of Reactive Red 120 dye adsorption by chitosan beads from aqueous solution, Energy, Ecology and Environment, 2 (2017) 85-93.
[57] H.M. Abdel-Aziz, R.S. Farag, S.A. Abdel-Gawad, Carbamazepine Removal from Aqueous Solution by Green Synthesis Zero-Valent Iron/Cu Nanoparticles with Ficus Benjamina Leaves' Extract, International Journal of Environmental Research, (2019) 1-10.
[58] W. Li, C. Guo, B. Su, J. Xu, Photodegradation of four fluoroquinolone compounds by titanium dioxide under simulated solar light irradiation, Journal of Chemical Technology & Biotechnology, 87 (2012) 643-650.
[59] M.R. Abukhadra, M.A. Sayed, A.M. Rabie, S.A. Ahmed, Surface decoration of diatomite by Ni/NiO nanoparticles as hybrid composite of enhanced adsorption properties for malachite green dye and hexavalent chromium, Colloids and Surfaces A: Physicochemical and Engineering Aspects, 577 (2019) 583-593.